Structure−Activity Relationships in the Oxidation of Para-Substituted Benzylamine Analogues by Recombinant Human Liver Monoamine Oxidase A[†,‡]

J. Richard Miller[§] and Dale E. Edmondson*[,||]

Departments of Biochemistry and Chemistry, Emory University, Atlanta, Georgia 30322-3050

Received April 22, 1999; Revised Manuscript Received August 2, 1999

ABSTRACT: Monoamine oxidase A (MAO A) plays a central role in the oxidation of amine neurotransmitters. To investigate the structure and mechanism of this enzyme, recombinant human liver MAO A was expressed and purified from *Saccharomyces cerevisiae*. Anaerobic titrations of the enzyme require only 1 mol of substrate per mole of enzyme-bound flavin for complete reduction. This demonstrates that only one redox-active group (i.e., the covalent FAD cofactor) is involved in catalysis. The reaction rates and binding affinities of 17 para-substituted benzylamine analogues with purified MAO A were determined by steady state and stopped flow kinetic experiments. For each substrate analogue that was tested, the rates of steady state turnover (k_{cat}) and anaerobic flavin reduction (k_{red}) are similar in value. Deuterium kinetic isotope effects on k_{cat}, k_{red}, k_{cat}/K_m, and k_{red}/K_s with α,α-[^{2}H]benzylamines are similar for each substrate analogue that was tested and range in value from 6 to 13, indicating that α-C−H bond cleavage is rate-limiting in catalysis. Substrate analogue dissociation constants determined from reductive half-reaction experiments as well as from steady state kinetic isotope effect data [Klinman, J. P., and Matthews, R. G. (1985) *J. Am. Chem. Soc. 107*, 1058−1060] are in excellent agreement. Quantitative structure−activity relationship (QSAR) analysis of dissociation constants shows that the binding of para-substituted benzylamine analogues to MAO A is best correlated with the van der Waals volume of the substituent, with larger substituents binding most tightly. The rate of para-substituted benzylamine analogue oxidation and/or substrate analogue-dependent flavin reduction is best correlated with substituent electronic effects (σ). Separation of the electronic substituent parameter (σ) into field-inductive and resonance effects provides a more comprehensive treatment of the electronic correlations. The positive correlation of rate with σ ($\rho \sim 2.0$) suggests negative charge development at the benzyl carbon position occurs and supports proton abstraction as the mode of α-C−H bond cleavage. These results are discussed in terms of several mechanisms proposed for MAO catalysis and with previous structure−activity studies published with bovine liver MAO B [Walker, M. C., and Edmondson, D. E. (1994) *Biochemistry 33*, 7088−7098].

Monoamine oxidases A and B (MAO A[1] and MAO B, respectively, EC 1.4.3.4) catalyze the oxidation of primary, secondary, and some tertiary amines to their corresponding protonated imines with concomitant reduction of O_2 to hydrogen peroxide (*1*). The dissociated imine product is then nonenzymatically hydrolyzed to the corresponding aldehyde (*2*, *3*). Monoamine oxidases are flavoproteins localized to the outer mitochondrial membranes of mammals, birds, fish, and a variety of lower animals and some fungi (*4*). Two isoforms, MAO A and MAO B, are found in humans and other mammals. The amino acid sequences of the two human isoforms are 71% identical (*5*), and each contains a FAD cofactor covalently attached to a conserved cysteinyl residue via an 8-α-*S*-thioether linkage (*6*). MAO A and MAO B have received extensive attention as antidepressants. MAO B inhibitors are currently used synergistically with L-DOPA therapy in the treatment of Parkinson's disease (*7*). Despite an extensive literature on these two enzymes, the detailed mechanism by which they catalyze amine oxidation is not well-defined, although several mechanisms have been proposed. Previous work in this laboratory has probed the structure and mechanism of bovine liver MAO B by examining the influence of para and meta substitution of benzylamine on its binding and kinetic properties (*2*, *8*). This paper extends these studies to recombinant human liver MAO A with the expectation that clear differences might be found between the two enzymes that would be valuable in future drug development.

The reductive half-reaction of MAO A (*9*), as also found with MAO B (*10*), exhibits kinetic behavior which follows

[†] This work was supported by Grant GM-29433 from the National Institutes of Health (to D.E.E.). J.R.M. was partially supported by a predoctoral Cell and Molecular Biology Training Grant from the NIH (GM-08367).

[‡] A preliminary account of this work was presented at the Isotopes in Biological and Chemical Sciences Gordon Conference, Ventura, CA, January 1998.

* To whom correspondence should be addressed: Department of Biochemistry, Emory University School of Medicine, Rollins Research Center, 1510 Clifton Rd., Atlanta, GA 303222-3050. E-mail: dedmond@bimcore.emory.edu. Phone: (404) 727-5972. Fax: (404) 727-2738.

[§] Department of Biochemistry. Present address: Department of Biological Chemistry, The University of Michigan, Ann Arbor, MI 48109.

[||] Departments of Biochemistry and Chemistry.

[1] Abbreviations: MAO, monoamine oxidase; DOPA, dihydroxyphenylalanine; E_{ox}, oxidized enzyme; E_{red}, reduced enzyme; SET, single-electron transfer; EPR, electron paramagnetic resonance; QSAR, quantitative structure−activity relationships.

10.1021/bi990920y CCC: $18.00
Published on Web 09/24/1999

Scheme 1: Kinetic Mechanism of MAO A[a]

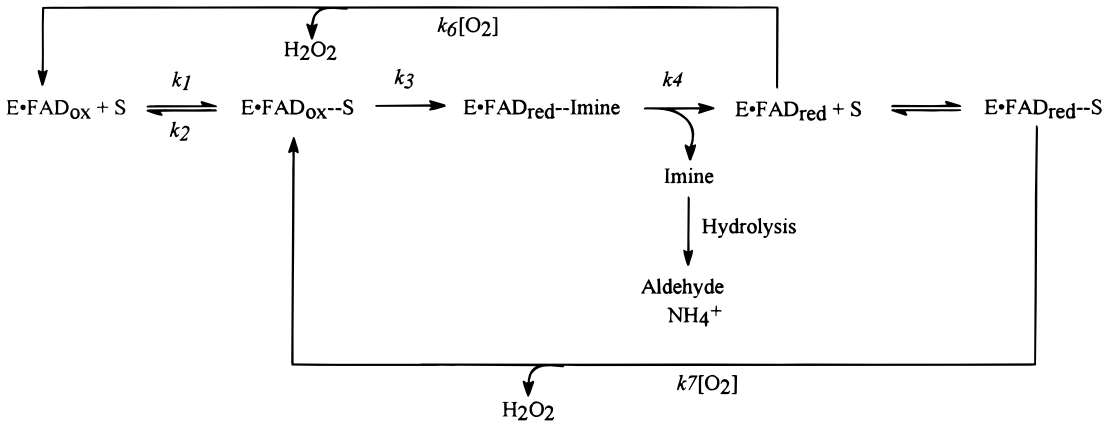

[a] From ref *9*.

Scheme 2: Proposed Aminium Cation Radical Mechanism for MAO A Catalysis[a]

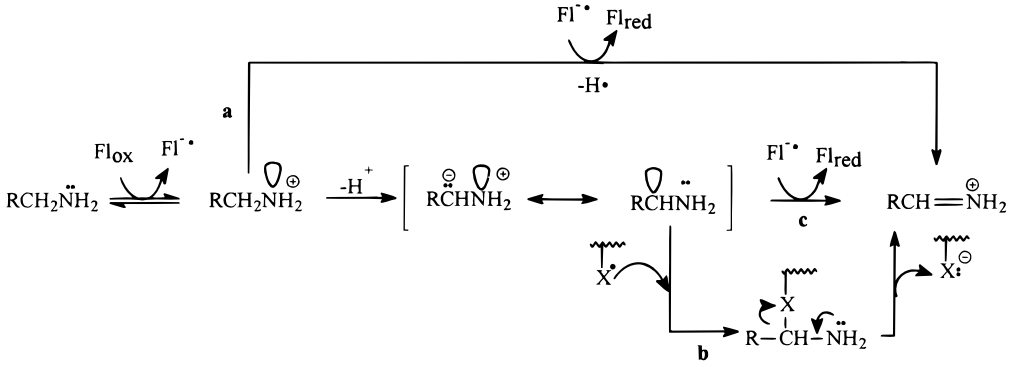

[a] From ref *15*.

that described by Strickland et al. (*11*). Comparative studies of MAO A purified from human placenta (*12*) and of recombinant human liver enzyme purified from yeast (*9*, *13*) suggest a similar kinetic mechanism (Scheme 1). One unusual property of MAO A that has not yet been resolved is the fact that the rate of flavin reduction determined from stopped flow kinetic studies is slower than the turnover number found in steady state kinetic studies (*14*). Ramsey and co-workers have suggested several explanations for this unusual behavior, but none of these have been experimentally verified. MAO A does differ from MAO B in that it is less active with benzylamine substrates and has a much lower $K_m(O_2)$ (~6 and 240 μM, respectively) (*9*).

Several mechanisms have been proposed for MAO B catalysis on the basis of the work with purified enzyme and chemical model systems. Since MAO A is highly homologous with MAO B and both enzymes have identical flavin cofactors, an unwritten assumption in the literature is that both enzymes function by similar chemical mechanisms. The most widely quoted mechanism for MAO B catalysis, originally proposed by Silverman and colleagues, involves an aminium cation radical intermediate (*15*) (Scheme 2) which is formed via an initial single-electron transfer (SET) from the amine nitrogen to the oxidized flavin cofactor which produces an aminium cation radical and flavin semiquinone. Several possibilities for α-hydrogen abstraction could follow (Scheme 2). The basis for this mechanism is derived from SET chemistry observed in electrochemical and chemical oxidations of amines (*15*) and in the observed inactivation of MAO B upon incubation with highly reactive amine substrate analogues known to undergo SET chemistry and ring opening in model reactions (*16*).

A polar nucleophilic mechanism originally proposed by Hamilton (*17*) has received further support from the model system work of Mariano and colleagues (*18*). MAO catalysis is proposed to occur via nucleophilic attack at the flavin 4a position by the deprotonated amine (Scheme 3). Proton abstraction from the α-carbon of the amine−flavin 4a adduct is proposed to be facilitated by an active site base on the enzyme. Formation of the protonated imine product results from its elimination from the reduced flavin. Support for this mechanism comes from the observed oxidative deamination of benzylamine in the presence of *N*(3)-methyllumiflavin (*18*). Additionally, primary and secondary amines are observed to readily form stable 4a adducts with *N*(5)-ethyl-*N*(3)-methyllumiflavinium perchlorate which can then undergo base-catalyzed elimination to the corresponding imine and reduced flavin (*19*).

A third mechanism proposed for MAO B catalysis was based on results obtained in this laboratory (*8*, *20*). This mechanism suggests that α-C−H bond cleavage occurs via a direct hydrogen atom transfer from the amine α-carbon to a protein-based non-flavin radical with subsequent electron transfer to the flavin. Evidence supporting this mechanism comes from several sources. Quantitative structure−activity relationships (QSAR) derived from the reaction rates of a series of para- and meta-substituted benzylamine analogues with MAO B show no apparent dependence of the limiting rate of flavin cofactor reduction on the electronic properties of the substituents (*8*). Second, an organic radical species is

Scheme 3: Proposed Polar Nucleophilic Mechanism for MAO Catalysis[a]

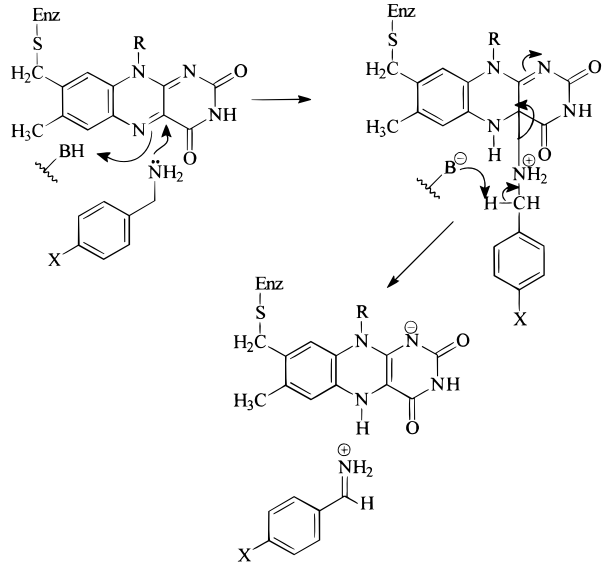

[a] From ref *18*.

observed in EPR spectra of resting bovine liver MAO B (*21*, *22*). This species could be sufficiently reactive to abstract an α-hydrogen atom from the amine substrate.

Recent unpublished evidence from this laboratory, however, does not support the presence of a stable radical species of catalytic significance in either MAO B or MAO A. Highly purified recombinant human liver MAO B expressed in the methylotrophic yeast *Pichia pastoris* and purified recombinant human liver MAO A expressed in *Saccharomyces cerevisiae* exhibit no detectable EPR signals in their respective resting states (P. N. Vinson, R. K. Nandigama, and D. E. Edmondson, unpublished results). The absence of an EPR signal in these fully functional enzyme preparations does not support the involvement of a stable amino acid (*8*, *21*) or flavin (*22*) radical in MAO catalysis. The radical species observed in bovine liver MAO B is likely an artifact of the purification procedure.

Quantitative structure−activity relationships are useful as mechanistic probes of reaction mechanisms in both organic chemistry and enzymology (*23*). Reaction rates and/or binding data for a series of closely related substrates containing one or more substituents can be analyzed according to the following equation:

$$\log k \text{ (or } K_d) = \rho(\sigma) + A(\pi) + B(V_w) \text{ (or } E_s) + C \quad (1)$$

where σ refers to the electron donating or withdrawing properties of the substituent (*23*), π describes the lipophilicity of the substituent (*24*), and V_w and E_s are steric terms, the van der Waals volume (*25*) and Taft steric parameter (*26*), respectively. Several examples of the successful application of this mechanistic approach to enzymatic reactions include the quinoproteins, plasma amine oxidase (*27*), methylamine dehydrogenase (*28*), and aromatic amine dehydrogenase (*29*), as well as the flavoproteins, MAO B (*8*), D-amino acid oxidase (*30*), and lactate oxidase (*31*).

This study reports kinetic and spectroscopic approaches to probing the catalytic mechanism of recombinant human liver monoamine oxidase A. Anaerobic reductive titrations of the enzyme show only 1 equiv of substrate is required for full reduction, which does not support the involvement of a redox-active disulfide group, in addition to the flavin (*32*), in MAO catalysis. Stopped flow and steady state kinetic studies using a variety of para-substituted benzylamine analogues comprise the first extensive QSAR analysis of purified recombinant human liver MAO A. The reaction rates and binding affinities of 17 different para-substituted benzylamine analogues with the enzyme were determined and show a strong correlation between the rate of flavin reduction and the electron withdrawing properties of the substituent. These results suggest proton abstraction as the mode of C−H bond cleavage in the MAO A-catalyzed oxidation of benzylamine. The relevance of these results to the three proposed mechanisms of MAO catalysis is discussed. The binding and rate structure−activity correlations observed for MAO A differ significantly from those found previously with MAO B (*8*). Possible reasons for these differences are discussed.

EXPERIMENTAL PROCEDURES

Expression and Purification of Monoamine Oxidase A. Recombinant human liver monoamine oxidase A was expressed in *S. cerevisiae* strain RH218 as described previously (*33*), except two 12 L fermenters (New Brunswick Scientific) were utilized for cell growth and induction. Purification of MAO A followed the procedure described previously (*34*). Typical enzyme yields from 22 L of yeast culture resulted in 50−120 mg of pure MAO A with a specific activity of 1.5 ± 0.5 units of MAO A/mg of protein (units defined below).

Prior to use, the purified enzyme was concentrated 20-fold under nitrogen in an Amicon stirred cell and then diluted 20-fold using 50 mM potassium phosphate (pH 7.5) and 0.8% (w/v) octyl β-D-glucopyranoside (enzyme buffer). Twenty-fold concentration of the enzyme was repeated, followed by addition of enzyme buffer to give an appropriate enzyme concentration.

Enzyme Assays. Standard assays of MAO A activity were conducted spectrophotometrically using a Gilford update of a Beckman model DU spectrophotometer. Assays were conducted at 30 °C in 50 mM potassium phosphate (pH 7.5), 5 mg/mL reduced Triton X-100, and 236 μM O_2 (air saturation). Each assay solution contained 1 mM kynuramine. The rate of MAO A-catalyzed oxidation of kynuramine to 4-hydroxyquinoline was calculated from the increase in absorbance at 316 nm using an extinction coefficient of 12 300 M^{-1} cm^{-1} (*12*). One unit of enzyme activity is defined as the amount of enzyme required to oxidize 1 μmol of kynuramine in 1 min. The concentration of active enzyme was determined using a turnover number of 125 min^{-1} at saturating kynuramine concentrations (*12*).

Anaerobic Titrations of MAO A. The percent functionality and concentration of the enzyme were measured by spectral monitoring of the level of enzyme-bound flavin reduction during anaerobic titrations of the enzyme with *p*-chlorobenzylamine and sodium dithionite as described previously (*8*). Typical percent functionality varied from 80 to 97%.

Substrate Analogues. All reagents were from Aldrich, Pfaltz, and Bauer, Inc., or TransWorld Chemical. Both α,α-[^{1}H]- and α,α-[^{2}H]-para-substituted benzylamine hydrochlorides were prepared by reduction of the corresponding

benzonitriles as described previously (*8*). Efficient synthesis of α,α-[^{1}H]- and α,α-[^{2}H]-*p*-iodobenzylamine required the addition of equimolar amounts of aluminum chloride (*35*) prior to the addition of reductant. *p*-Isopropyl-, *p*-hydroxy-, and *p*-acetylbenzylamine analogues were synthesized as described by Hartman and Klinman (*27*). The purity of each analogue was confirmed by ^{1}H NMR (GE 300 MHz instrument) and low-resolution fast atom bombardment mass spectrometry. Para-substituted α,α-dideuterated benzylamine analogues showed no detectable NMR signal from the methylene protons, indicating >98% deuterium incorporation.

Steady State Kinetic Measurements of Para-Substituted Benzylamine Analogue Oxidation. The steady state rate of benzylamine oxidation to the corresponding aldehyde was measured spectrophotometrically. Assays were conducted at 10.9 °C in enzyme buffer with 337 μM O_2 (air saturation). This temperature was used since preliminary experiments showed the enzyme preparations to be unstable to prolonged incubation at 25 °C which is required for stopped flow kinetic experiments. Rates were measured with at least eight different amine concentrations (25 μM to 8 mM) spanning more than 2 orders of magnitude. Detection wavelengths and molar absorption extinction coefficients for each aldehyde were used as given by Walker and Edmondson (*8*). The concentration of MAO A in each assay ranged from 0.36 to 2.2 μM, depending on the oxidation rate and aldehyde extinction coefficient of each substrate. Steady state kinetic isotope effects with α,α-[^{1}H]- and α,α-[^{2}H]benzylamine analogues were calculated from reaction rates determined at the same enzyme concentration. Michaelis−Menten kinetic behavior was observed for all amine analogues for which steady state kinetic data are reported.

Enzyme-Monitored Turnover Experiments. Experiments were conducted using a single-wavelength stopped flow apparatus (Kinetic Instruments, Ann Arbor, MI) with a dead time of 1 ms and a cell path length of 2 cm. Air-saturated solutions of MAO A (variable concentrations) and *p*-trifluoromethylbenzylamine (5 mM) were mixed, and the change in flavin absorbance at 450 nm was monitored and recorded using a Nicolet 4094 digital oscilloscope. Reaction rates were determined by manual integration of absorbance versus time plots as described previously (*36*).

Single-Wavelength Anaerobic Stopped Flow Kinetic Experiments. Experiments were conducted using the stopped flow spectrophotometer described above. The entire flow line of the apparatus was made anaerobic by incubation with argon-purged enzyme buffer containing 50 mM glucose, 22 nM glucose oxidase, and 100 units/mL catalase for at least 2 h prior to experiments. Solutions of MAO A (10 μM) and benzylamine analogue (minimum of 100 μM in enzyme buffer) were placed in tonometers and made anaerobic as described above. After mixing, changes in absorbance at 450 nm were recorded using a Nicolet 4094 digital oscilloscope. The data files were transferred to a Dell 386 computer for subsequent analysis.

The apparent pseudo-first-order rate of flavin reduction with each amine was determined at a minimum of six different amine concentrations spanning at least 2 orders of magnitude. The apparent rate constant of flavin reduction at each amine concentration was measured in triplicate.

Anaerobic Rapid-Scanning Stopped Flow Kinetic Experiments with α,α-[^{1}H]- and α,α[^{2}H]-p-Chlorobenzylamine. Conditions and preparation of anaerobic enzyme and substrates were identical to that described for single-wavelength stopped flow experiments except that 25 μM MAO A was utilized. Experiments were conducted using an OLIS-RSM1000 stopped flow spectrophotometer (OLIS, Inc., Bogart, GA) in the laboratory of W. David Wilson (Department of Chemistry, Georgia State University, Atlanta, GA). Spectra were acquired across a 150 nm range from 335 to 485 nm.

Data Analysis. Steady state kinetic data were fit to the Michaelis−Menten equation using a nonlinear least-squares fitting routine incorporated into the Origin software package (Microcal Software). Stopped flow data were similarly fit using an equation corresponding to a single-exponential decay with an offset. Determination of limiting rates of flavin reduction and dissociation constants for each amine substrate was performed as described by Strickland (*11*), using the Origin software package. Fits to the data were confirmed by reanalysis using the GraFit software package (Erithacus Software). Analysis of rapid-scanning stopped flow data was conducted using the Global Fit algorithm (*37*) resident in the OLIS RSM-1000 software package.

Values of substituent parameters (σ, π, and E_s) were obtained from Hansch et al. (*26*). Values for the van der Waals volume (V_w) of each substituent were calculated as described by Bondi (*25*). Multivariate linear regression analysis of rate and binding data as a function of substituent parameters was performed using the StatView software package (Abacus Concepts).

RESULTS

Anaerobic Reductive Titration of MAO A. A requirement for analysis of substituent effects on the steady state rate of MAO A catalysis and anaerobic flavin reduction rates is that the stoichiometry of the reaction be known. A recent report by Sablin and Ramsay (*32*) suggested, on the basis of reductive titrations of MAO A with dithionite, that four reducing equivalents are required for full reduction of the enzyme. These were suggested to be distributed as two reducing equivalents to the covalent flavin and two reducing equivalents to a redox-active disulfide in the enzyme. It was further proposed that the pathway for electron transfer from the amine to the flavin involves this putative redox-active disulfide as an intermediary by an undefined mechanism. If such a scheme were operative, then 2 mol of substrate would be required to reduce MAO A rather than 1 where the first mole of substrate would result in little or no flavin reduction since disulfide bonds typically exhibit a lower potential than flavins. Flavin reduction would commence on the addition of the second mole of substrate and would be readily monitored by its change in visible absorbance. To test this hypothesis, an anerobic solution of recombinant human liver MAO A (17.2 μM) was reduced by successive additions of an anaerobic solution of *p*-chlorobenzylamine. After the addition of each aliquot of substrate, the enzyme solution was allowed to equilibrate, and then a visible absorbance spectrum was recorded (Figure 1). The rate of reduction of the enzyme-bound flavin is found to be linearly dependent on the amount of *p*-chlorobenzylamine added and a stoichi-

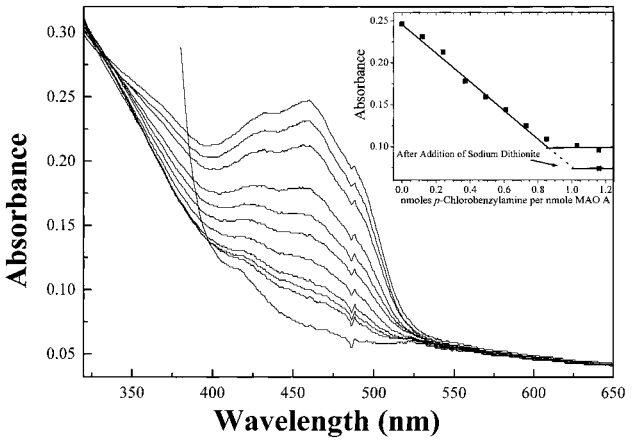

FIGURE 1: Reductive titration of recombinant human liver MAO A by *p*-chlorobenzylamine requires 1 mol of substrate (two electron equivalents). MAO A (17.2 μM, in enzyme buffer) was reduced by successive additions of an anaerobic solution of *p*-chlorobenzylamine at 10.9 °C. The visible absorbance spectrum of the enzyme is shown after the addition of each aliquot (from top, in mole per mole of enzyme−flavin, 0, 0.12, 0.24, 0.37, 0.49, 0.61, 0.73, 0.85, 1.03, 1.16) and after the addition of several crystals of sodium dithionite (bottom spectrum). The inset shows a plot of the change in absorbance at 456 nm as a function of the molar ratio of added *p*-chlorobenzylamine to enzyme. The end point of the titration and the absorbance reached after the addition of sodium dithionite are shown.

ometry of 1.1 mol of substrate (two electron equivalents) for each mole of active enzyme was required for full reduction (inset of Figure 1). Reduction of the small amount of remaining inactive enzyme was accomplished by addition of sodium dithionite. Approximately 84% of the enzyme shown in Figure 1 can be reduced by substrate. Similar results were obtained when a separate enzyme preparation was quantitatively reduced with tyramine (data not shown). To confirm the stoichiometry observed by anaerobic titration with substrate, recombinant human liver MAO A was titrated separately with the irreversible inhibitor clorgyline. Complete inactivation of an identical sample of the enzyme utilized in Figure 1 required approximately 1.3 mol of clorgyline per mole of active enzyme (data not shown).

These results clearly show that reduction of MAO by substrate requires only two electron equivalents. Furthermore, no spectrally detectable intermediates such as flavin semiquinone are observed during the reductive titration of the enzyme. This apparent discrepancy with the dithionite titrations published by Sablin and Ramsay can be attributed to the nonspecific reduction of protein-bound disulfides by dithionite, which is shown to occur in the case of xanthine oxidase (*38*), or, alternately, to the slow kinetic equilibration of MAO A with dithionite which might complicate the interpretations of reductive titrations with that reagent.

Steady State Kinetic Behavior of the MAO A-Catalyzed Oxidation of Ring-Substituted α,α-*[^{1}H]- and* α,α-*[^{2}H]-Benzylamine Analogues.* Steady state kinetic parameters for the oxidation of seven para-substituted benzylamine analogues by MAO A were determined and the results shown in Table 1. All kinetic assays were conducted at 10.9 °C due to the thermal lability of the enzyme above 15 °C. Turnover numbers were calculated at saturating amine concentrations, and air-equilibrated buffers were found to be saturating in oxygen since MAO A has a low $K_m(O_2)$ (~6 μM) (*9*).

Table 1: Steady State Kinetic Constants for the MAO A-Catalyzed Oxidation of Para-Substituted Benzylamine Analogues[a]

para substituent	k_{cat}(H) (min^{-1})	$^Dk_{cat}$	K_m(H) (μM)	K_m(D) (μM)	$^D(k_{cat}/K_m)$
H	2.54 ± 0.08	11.5 ± 0.6	1040 ± 150	1100 ± 120	12.1 ± 2.3
CF_3	85.1 ± 1.7	8.1 ± 0.2	634 ± 55	881 ± 65	11.3 ± 1.3
Br	17.2 ± 0.5	9.6 ± 0.4	157 ± 21	157 ± 17	9.6 ± 1.7
Cl	15.2 ± 0.5	9.8 ± 0.4	231 ± 20	178 ± 30	7.5 ± 1.7
F	7.55 ± 0.38	8.2 ± 0.3	958 ± 110	1110 ± 80	9.5 ± 1.3
MeO	1.56 ± 0.03	12.9 ± 0.7	106 ± 8	80 ± 16	9.8 ± 2.2

[a] All measurements were conducted at 10.9 °C in air-saturated enzyme buffer.

The turnover numbers [k_{cat}(H)] calculated for each substrate analogue exhibit a marked dependence on the nature of the substituent, with values spanning a more than 50-fold range (from 1.56 min^{-1} for *p*-methoxybenzylamine to 85 min^{-1} for *p*-trifluoromethylbenzylamine). Comparison of the observed rates of para-substituted benzylamine oxidation to those previously observed with MAO B (*8*) shows that with the exception of *p*-trifluoromethylbenzylamine, MAO A oxidizes these amine analogues more slowly than does MAO B.

Previous kinetic studies of bovine liver MAO B have shown that deuterium substitution of the α-protons of benzylamine analogues results in large kinetic isotope effects on the steady state turnover rate ($^Dk_{cat}$ ranges from 6.0 to 8.9) (*8*, *10*). Examination of the same α,α-[^{2}H]benzylamine analogues with recombinant human liver MAO A also shows large isotope effects ($^Dk_{cat}$ ranges from 8.2 to 12.9) (Table 1). Isotope effects on k_{cat}/K_m are similar to those observed on k_{cat}. The magnitudes of these effects demonstrate that α-C−H bond cleavage is rate-limiting with all tested analogues in MAO A steady state turnover. The steady state kinetic isotope effect data (Table 1) also allow estimation of substrate dissociation constants representing all preisotopically sensitive equilibria (*39*). Dissociation constants for each benzylamine analogue were calculated from the data in Table 1 according to the following equation:

$$\frac{^Dk_{cat} - 1}{^D(k_{cat}/K_m) - 1} = K_m/K_d \qquad (2)$$

The calculated K_d values, shown in Table 2, differ from the experimentally determined K_s values by less than a factor of 2.

Effect of the Para Substituent on the Reductive Half-Reaction of MAO A with Benzylamine Analogues. The large $^Dk_{cat}$ values (Table 1) support the view that α-C−H bond cleavage is the rate-limiting step in catalysis of all substituted benzylamine analogues, which allows correlations of steady state data with substituent parameters. More definitive kinetic data for use in structure−activity correlations can be obtained from a determination of the rates of enzyme reduction in reductive half-reaction experiments using anaerobic stopped flow techniques. Moreover, this approach allows the determination of binding constants and limiting rates of flavin reduction for the analogue being investigated as outlined by Strickland et al. (*11*) and applied previously to MAO A by Ramsay (*9*). Plots of $1/k_{obs}$ versus 1/[amine] are linear for all of the analogues tested and exhibit finite *y* intercepts. These properties demonstrate that $k_2 \gg k_3$ and $k_3 \gg k_4$ (eq

Table 2: Effects of Para Substituents on the Rates of Flavin Reduction by Benzylamine Analogues and Their Respective Binding Affinities with MAO A

para substituent	k_{red}(H) (min^{-1})	k_{red}(D) (min^{-1})	$^{D}k_{red}$	K_s(H)[a] (μM)	K_s (D)[a] (μM)	K_d[e] (μM)	$^{D}(k_{red}/K_s)$
H	1.42 ± 0.20	0.16 ± 0.02	9.3 ± 1.2	18.1 ± 2.3	ND	16.8	
CF_3	40.1 ± 2.2	4.53 ± 0.30	8.9 ± 0.8	35.1 ± 1.8	42.6 ± 6.4	49	10.8 ± 1.9
Br	11.7 ± 0.6	1.53 ± 0.06	7.7 ± 0.5	2.54 ± 0.23	2.15 ± 0.36	4.0	6.5 ± 1.3
Cl	7.94 ± 0.30	0.90 ± 0.05	8.9 ± 0.6	6.28 ± 0.11	4.69 ± 0.41	4.4	6.6 ± 0.7
Me	3.11 ± 0.20	0.36 ± 0.02	8.6 ± 0.7	2.01 ± 0.21	ND	2.2	
F	2.92 ± 0.20	0.33 ± 0.03	8.8 ± 0.9	17.9 ± 2.6	19.9 ± 3.9	19	9.8 ± 2.6
MeO	0.75 ± 0.06	<0.1	>8	0.91 ± 0.23	ND	0.54	
EtO	1.73 ± 0.10	ND		1.45 ± 0.39	ND		
NO_2	12.4 ± 0.7	ND		69.9 ± 12.1	ND		
$N(CH_3)_2$[b]	2.43 ± 0.21	0.16 ± 0.06	11.6 ± 3.4	0.64 ± 0.15	ND		
$N(CH_3)_2$[c]	1.94 ± 0.04	0.17 ± 0.02	11.4 ± 1.4	0.43 ± 0.03	ND		
$CH(Me)_2$	1.95 ± 0.06	ND		1.28 ± 0.20	ND		
CF_3O	26.0 ± 0.8	3.68 ± 0.12	7.1 ± 0.3	9.39 ± 1.47	10.8 ± 1.4		8.1 ± 1.7
I	16.8 ± 0.3	2.88 ± 0.05	5.8 ± 0.2	1.59 ± 0.13	2.11 ± 0.16		7.7 ± 0.9
n-butyl	1.85 ± 0.03	ND		0.36 ± 0.02[d]	ND		
tert-butyl	~0.1	ND		1.33 ± 0.01[d]	ND		
OH	3.44 ± 0.18	ND		7.84 ± 1.60	ND		
acetyl	11.1 ± 0.4	ND		122 ± 14	ND		

[a] K_s values are corrected for selective binding of the deprotonated amine according to eq 4b. [b] Rate of flavin reduction. [c] Rate of protonated *p*-*N*,*N*-dimethylbenzylimine formation. [d] Values of K_i for the competitive inhibition of *p*-trifluoromethylbenzylamine oxidation. [e] Values are calculated from steady state kinetic isotope effect data in Table 1 as described by Klinman and Matthews (*39*) and eq 2. Data marked ND were not determined due to the slow reaction rates of these substrates. All reactions were conducted at 10.9 °C in air-saturated enzyme buffer.

3). Therefore, $K_s = k_2/k_1$, and the limiting rate of enzyme reduction (k_{red}) is equivalent to k_3 in eq 3 (*11*).

$$E + S \underset{k_2}{\overset{k_1}{\rightleftharpoons}} ES \underset{k_4}{\overset{k_3}{\rightleftharpoons}} E_{red}-imine \xrightarrow{k_5} E_{red} + imine \qquad (3)$$

The limiting rates of reduction of the MAO A flavin cofactor by 17 different α,α-[^{1}H] and 11 α,α-[^{2}H] para-substituted benzylamine analogues were determined. Those analogues not used in steady state kinetic experiments either were too slow for convenient steady state analysis or did not lend themselves to convenient spectral monitoring of initial rates. The concentration of amine substrate was always at least 10-fold higher than that of the enzyme to ensure pseudo-first-order kinetic behavior. Rates of flavin reduction (k_{obs}) were determined from the change in flavin absorbance at 450 nm.

The values of k_{red} determined for each benzylamine analogue (Table 2) are found to be consistently lower than their corresponding steady state turnover numbers (Table 1) (the ratio of k_{cat} to k_{red} is 2.1 ± 0.4). This behavior has been observed previously by Ramsay et al. (*14*), who suggested several possible explanations but provided no experimental support for them. A reasonable source of this behavior might be due to aggregation of the detergent-solubilized enzyme at the higher concentrations of enzyme required for stopped flow experiments. To investigate this possibility, the rate of MAO A-catalyzed oxidation of *p*-trifluoromethylbenzylamine was determined as a function of enzyme concentration using enzyme-monitored turnover techniques (Figure 2) (*36*). The apparent rate of *p*-trifluoromethylbenzylamine oxidation is inversely correlated with enzyme concentration (Figure 2). Extrapolation of the observed rate of *p*-trifluoromethylbenzylamine turnover to infinite enzyme dilution results in an extrapolated turnover number (75−85 min^{-1}) that is comparable to the steady state rate observed at enzyme concentrations of less than 1 μM (85.1 ± 1.7 min^{-1}). At an enzyme concentration of 5 μM, the turnover number calculated from

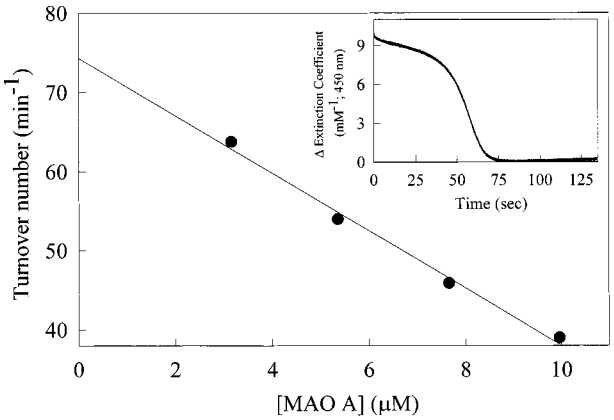

FIGURE 2: Dependence of the turnover number of MAO A-catalyzed oxidation of *p*-trifluoromethylbenzylamine on enzyme concentration. Reaction rates were determined at the indicated concentrations of MAO A in enzyme buffer using enzyme-monitored stopped flow turnover techniques. The substrate concentration is 5 mM (after mixing) in enzyme buffer, and O_2 is present at air saturation at 10.9 °C (337 μM). The inset shows the time-dependent change in the visible absorbance of the MAO A flavin cofactor. The concentration of MAO A is 16 μM prior to mixing with an equal volume of 10 mM *p*-trifluoromethylbenzylamine.

enzyme-monitored turnover experiments is comparable to the limiting rate of flavin reduction observed in anaerobic stopped flow reactions. To control for the systematic effect of enzyme concentration on reaction rates, the concentration of MAO A in all anaerobic stopped flow experiments was maintained at 5 μM.

A 50-fold range of k_{red} is observed with the substrate analogues that were examined, *p*-methoxybenzylamine being the slowest and *p*-trifluoromethylbenzylamine being the most rapid (Table 2). The K_s values that were determined span a more than 100-fold range with those analogues containing large, bulky substituents binding to MAO A with the highest affinity. These K_s values differ significantly from those previously observed for MAO B, although the range of values is similar.

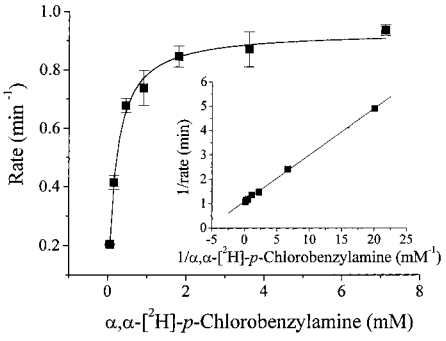

FIGURE 3: Dependence of the observed rate of anaerobic MAO A flavin reduction on α,α-[^{2}H]-*p*-chlorobenzylamine concentration. Apparent rates were measured at 10.9 °C, and all solutions were made using enzyme buffer. Rate values are the average of at least four separate determinations and are shown as the mean ± the standard error. Data were fit using a nonlinear least-squares method to the equation $y = ax/(b + x)$ (*11*). The inset shows reciprocal plots of rate dependence on amine concentration. Data were fit by a linear least-squares regression analysis.

Effects of α,α-Dideuteration of Benzylamine Analogues on the Reductive Half-Reaction of MAO A. The k_{red} values observed with α,α-[^{2}H]benzylamine analogues in anaerobic stopped flow experiments exhibit large kinetic isotope effects ($^Dk_{red}$ ranges from 5.8 to 11.6) (Table 2), indicating that, in agreement with the steady state data listed in Table 1, α-C−H bond cleavage is significantly rate-limiting in catalysis. The values of $^D(k_{red}/K_s)$ observed are similar to the corresponding values of $^Dk_{red}$. The values of $^Dk_{red}$ (combined primary and secondary kinetic isotope effects) with MAO A are similar in magnitude to those observed with bovine liver MAO B (*8*). The magnitudes of these isotope effects suggest that the values of k_{red} reflect the intrinsic rate of α-C−H bond cleavage (*40*).

Absence of Detectable Spectral Intermediates in Rapid-Scanning Stopped Flow Kinetic Traces. The use of a rapid-scanning stopped flow apparatus allows the collection of time-resolved absorption spectra during anaerobic reduction of MAO A by α,α-[^{1}H]- and α,α-[^{2}H]-*p*-chlorobenzylamine (Figure 4). Rapid-scanning spectral traces recorded at saturating substrate concentrations reveal a monophasic reduction of the FAD cofactor of MAO A (Figure 4). No evidence for the formation of any spectrally detectable intermediate (including the formation of either anionic or neutral flavin semiquinone or a flavin 4a adduct) is observed. Global fit analysis (*37*) of absorbance versus wavelength and time showed that oxidized flavin is the only chromophore undergoing a time-dependent change in absorbance (data not shown). Thus, if a chromogenic intermediate is formed during the reduction of MAO A, its concentration must be less than 5% of the sum of the concentrations of oxidized and reduced flavin to escape detection. These results are consistent with rapid-scanning stopped flow experiments previously reported for bovine liver MAO B (*41*).

Quantitative Structure−Activity Relationships Describing the Binding of Para-Substituted Benzylamine Analogues to MAO A. Binding constants for the binding of para-substituted benzylamine analogues to MAO A are shown in Tables 1 and 2. These include K_s values determined from anaerobic stopped flow studies with para-substituted α,α-[^{1}H]- and α,α-[^{2}H]benzylamines as well as K_d values calculated from steady state isotope effect data (see eq 2 above). To understand

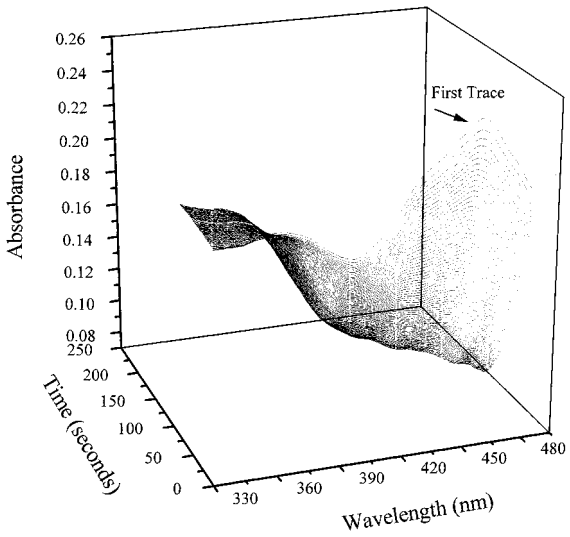

FIGURE 4: Rapid-scanning stopped flow spectral properties of the time course of the anaerobic reduction of MAO A (25 μM) with α,α-[^{2}H]-*p*-chlorobenzylamine (200 μM) in enzyme buffer. Reactions were conducted at 10.9 °C. Spectra were recorded at a rate of one per second using an OLIS-RSM1000 rapid-scanning stopped flow spectrophotometer.

which substituent properties best describe the binding of these substrates to MAO A, single and multiple variable linear regression analyses were performed using the experimentally determined binding constants (*26*). Binding data were fit to single- and/or multiple-parameter variations of eq 1. Initial statistical analysis of the MAO A binding data resulted in poor correlations with any of the substituent parameters. It should be noted that the determined K_d values were measured at pH 7.5 where the protonated forms of the amine analogues predominate. Since MAO A and MAO B have been suggested to bind only the deprotonated form of the substrate (*42, 43*), a correction of the observed binding constants to reflect the concentration of the deprotonated amine and also the influence of the substituent on the amine pK_a appeared to be necessary. The pK_a values of several para-substituted benzylamine analogues have been measured and exhibit a linear correlation of pK_a with σ and a negative ρ value (*44*):

$$pK_a = -1.03(\pm 0.07)\sigma + 9.31(\pm 0.02)$$
$$F_{1,9} = 226 \quad r = 0.98 \quad (4a)$$

This relationship allows the calculation of pK_a values for substituted benzylamine analogues whose pK_a values have not been experimentally determined. These considerations were used to calculate the dissociation constants of each deprotonated benzylamine analogue with MAO A using the following equation:

$$K_{d(corrected)} = \frac{K_{d(observed)}}{1 + \text{antilog}(pK_a - pH)} \quad (4b)$$

Corrected binding constants for each para-substituted benzylamine analogue used in this study are shown in Table 2.

Linear regression analysis using the pK_a-corrected values of K_s, K_d, and K_i results in two essentially parallel correlations of log K_d with the van der Waals volume (V_w) of the para substituent (Figure 5). Note that the values of V_w are scaled by a factor of 0.1 to make their values have magnitudes

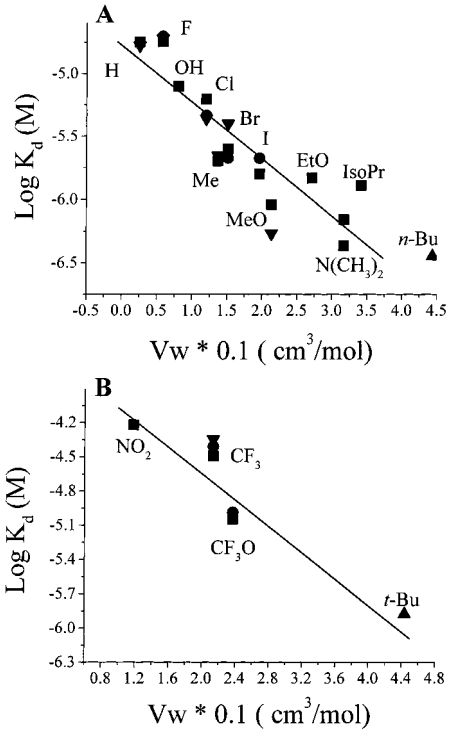

FIGURE 5: Correlations of the extent of binding of para-substituted benzylamines to MAO A with the van der Waals volume (V_w) of the para substituent. (A) Correlation of log K_d with V_w. Values of K_d are for α,α-diprotiobenzylamines (■) and α,α-dideuteriobenzylamines (●), with K_i constants from competitive inhibition of *p*-trifluoromethylbenzylamine oxidation (▲) and K_d values from steady state isotope effects (▼) (ref *39* and eq 2). (B) Correlation of log K_d of anomalous binding benzylamine analogues with V_w. Symbols are as described for panel A.

similar to those of the other substituent parameters. Most substituents (12) lie on a single line (Figure 5A, slope of -0.45 ± 0.05, correlation coefficient of 0.90). Four substituents (*p*-*tert*-butyl, *p*-trifluoromethoxy, *p*-trifluoromethyl, and *p*-nitrobenzylamine) exhibit anomalous behavior and could be grouped into a separate ("anomalous binding") curve (Figure 5B, slope of -0.60 ± 0.11, correlation coefficient of 0.93). Only *p*-acetylbenzylamine was not within a reasonable range of either curve and was not included in the binding analysis. The binding correlation of the anomalous substituents shown in Figure 5B represents only four substituents and is, therefore, less reliable than the correlation shown in Figure 5A. The slopes of the two correlations are identical within experimental error, suggesting the two plots reflect the same influence of para substituent on substrate binding affinity. A rationale for the presence of two separate binding correlations that differ only in the order of magnitude of the binding constants is not immediately apparent, although possible explanations are discussed below.

A statistical analysis of the substrate dissociation constant correlations is shown in Table 3. Correlations of MAO A binding data did not include the electronic substituent parameter (σ), since it is used in the calculation of amine pK_a values (eq 4a). The only single-parameter regression that shows a meaningful correlation with the substrate binding data is the van der Waals volume (V_w) of the substituent. For most of the substituents (Figure 5A), the regression analysis of log K_d with V_w exhibits a statistically high correlation with an $F_{1,21}$ value of 85 and a confidence level of >99.99%. For the four anomalous binding substituents shown in Figure 5B, the regression analysis for seven determinations exhibited an $F_{1,6}$ value of 31 and a confidence level of >99.7%. All other single-parameter correlations with the binding data exhibit poorer statistical correlations. Inclusion of the hydrophobic substituent parameter (π) or other parameters in the regression analysis of the data depicted in Figure 5A did not improve the statistical correlation. Not enough substituent data comprised the correlation in Figure 5B to justify inclusion of a second parameter. The similarity of the coefficient values for the correlations observed in both substituent groups suggests that the van der Waals volume is the best descriptor of benzylamine binding interactions in MAO A. The best mathematical description of the binding of the para-substituted benzylamine analogues (Figure 5A) to MAO A is

$$\log K_d = -0.45(\pm 0.05)V_w - 4.8(\pm 0.1) \qquad (5)$$

The binding of the four anomalous substituents (Figure 5B) to MAO A is best described by the equation

$$\log K_d = -0.60(\pm 0.11)V_w - 3.3(\pm 0.3) \qquad (6)$$

Effect of the Para Substituent on the Rates of Steady State Turnover and Flavin Reduction. Although the values of k_{cat} and k_{red} from Tables 1 and 2 likely reflect the same rate-limiting step in catalysis, the effect of enzyme concentration on reaction rate (Figure 2) results in k_{red} values that are 2-fold smaller than k_{cat} values. This difference requires that stopped flow and steady state rate data be analyzed separately.

Table 3: Correlations of the Binding Affinities (K_s or K_d) of Deprotonated Para-Substituted Benzylamines for MAO A with Steric, Electronic, and Hydrophobic Substituent Parameters[a]

parameter	correlation (slope)	*y*-intercept	correlation coefficient	F[c]	significance[d]
		K_d (12 substituents; lower curve in Figure 3)			
E_s[e]	0.67 ± 0.18	-4.8 ± 0.2	0.65	13	0.002
V_w	0.45 ± 0.05	-4.8 ± 0.1	0.90	85	<0.0001
π	-0.38 ± 0.18	-5.3 ± 0.1	0.41	4.3	0.05
$\pi + V_w$	0.13 ± 0.11 -0.49 ± 0.06	-4.8 ± 0.1	0.90	44	<0.0001
$\pi + E_s$[e]	-0.06 ± 0.29 0.61 ± 0.36	-4.8 ± 0.2	0.65	6.2	0.0094
		K_d[b] (4 substituents; upper curve in Figure 3)			
V_w	-0.55 ± 0.1	-3.5 ± 0.3	0.93	30	0.0030
π	-0.75 ± 0.21	-4.1 ± 0.2	0.84	12	0.018

[a] K_s values used in linear regression analysis were obtained from protio- and dideuteriobenzylamine analogues (Table 2). K_d values were calculated from the steady state isotope effects (Table 1) as described by Klinman and Matthews (*39*) and eq 2. All values are corrected to reflect the selective binding of deprotonated amine to the enzyme (*42*, *43*) and eq 4b. Correlations with the substituent electronic parameter (σ) were not determined due to its use in calculating amine pK_a values (eq 4a). [b] Correlations derived from four anomalous binding substituents (seven measurements). Correlations with E_s are not shown due to the lack of reliable E_s values for several substituents. [c] The F value is a statistical term relating the residuals of each point to the fitted line to the residuals of each point to the mean value. F is weighted for the number or variables in the correlation and the number of data points. A higher F indicates a better fit. [d] The significance is calculated from the F value and represents the fractional chance that the derived correlation is meaningless. [e] Correlations do not include *p*-*N*,*N*-(dimethylamino)- or *p*-ethoxybenzylamine due to the lack of reliable E_s values for these substituents.

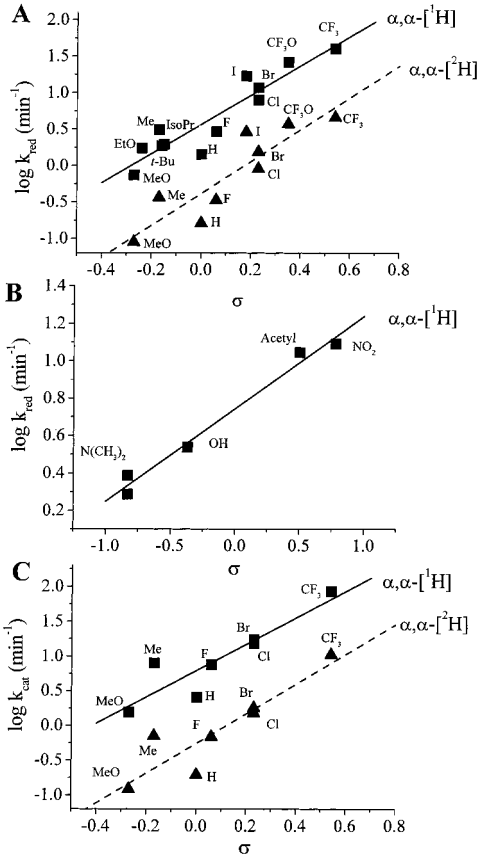

FIGURE 6: Correlation of steady state rates of MAO A turnover or anaerobic rates of MAO A flavin reduction with the substituent electronic parameter (σ). (A) Anaerobic rates of MAO A flavin reduction (k_{red}) by α,α-[^{1}H] (■) or α,α-[^{2}H] para-substituted benzylamines (▲). (B) Anaerobic rates of MAO A flavin reduction by anomalous-behaving benzylamine analogues. (C) Steady state rates (k_{cat}) with α,α-[^{1}H] (■) or α,α-[^{2}H] para-substituted benzylamines (▲).

Linear regression analysis of the rate of anaerobic flavin reduction (k_{red}) was conducted using a set of 16 substrate analogues. Twelve of these analogues exhibit a strong correlation of the rate of flavin reduction with the electronic substituent parameter (σ). The slope of this correlation (ρ value) is 1.8 ± 0.3 (correlation coefficient of 0.89, Figure 6A), indicating that electron-withdrawing substituents increase the rate of flavin reduction. The remaining four benzylamine analogues [*p*-nitro-, *p*-(dimethylamino)-, *p*-acetyl-, and *p*-hydroxybenzylamine] also exhibit a correlation of flavin reduction rates with σ. The ρ value observed with these four anomalous-behaving substituents is 0.50 ± 0.04 (correlation coefficient of 0.99, Figure 6B). In both cases, σ is the only single-substituent parameter that exhibits a strong correlation with reductive half-reaction rates of MAO A. The anomalous-behaving benzylamine analogues (Figure 6B) are unique in that these para substituents can serve as π-electron donors or acceptors. The influence of resonance stabilization may explain the different magnitudes of the ρ values. This idea will be discussed further in a later section.

Linear regression analysis of log k_{cat} as a function of substituent parameter shows a positive correlation with σ (ρ = 1.9 ± 0.4, correlation coefficient of 0.90, Figure 6C) and also with the steric parameter E_s (Table 4). Two parameter correlations of log k_{cat} values with both parameters improved the statistics of the correlation (Table 4) over other one- or two-parameter correlations. The significance of the steric contribution to the rate correlation is not observed in correlations of the rate of flavin reduction, and for the analogues used in steady state experiments (Table 1), a significant cross-correlation between σ and E_s substituent parameters is observed. These considerations make inclusion of the E_s parameter, as a predictor for influencing the rate of MAO A reduction, somewhat tenuous, whereas the electronic parameter of the substituent as a predictor is found in all analyses.

Table 4: Correlations of the Steady State Rate of MAO A Oxidation of Para-Substituted Benzylamines (k_{cat}) and the Limiting Rate of Flavin Reduction by Para-Substituted Benzylamines (k_{red}) with Steric, Hydrophobic, and Electronic Substituent Parameters[a]

parameter	correlation (slope)	*y*-intercept	correlation coefficient	*F*	significance
		k_{cat} (7 substituents)			
E_s	−0.66 ± 0.16	0.32 ± 0.19	0.88	18	0.0086
V_w	0.28 ± 0.34	0.60 ± 0.49	0.35	0.7	0.45
σ	1.89 ± 0.40	0.79 ± 0.11	0.90	23	0.005
π	0.66 ± 0.63	0.58 ± 0.42	0.42	1.1	0.35
$\sigma + E_s$	1.19 ± 0.31 −0.37 ± 0.11	0.50 ± 0.11	0.98	39	0.002
		k_{red} (12 substituents)			
E_s[b]	−0.48 ± 0.21	0.06 ± 0.3	0.63	5.3	0.050
V_w	−0.04 ± 0.15	0.75 ± 0.35	0.09	0.07	0.79
σ	2.01 ± 0.25	0.57 ± 0.06	0.93	63	<0.0001
π	0.056 ± 0.31	0.62 ± 0.31	0.06	0.03	0.86
		k_{red}[b] (5 anomalous substituents)			
V_w	−0.14 ± 0.20	0.98 ± 0.48	0.37	0.48	0.54
σ	0.50 ± 0.04	0.74 ± 0.03	0.99	170	0.001
π	−0.56 ± 0.44	0.54 ± 0.19	0.60	1.7	0.29

[a] Values of k_{cat} and k_{red} are from Tables 1 and 2, respectively. [b] Correlations with E_s reflect only the substrates for which reliable E_s values are available.

Analysis of the limiting rates of MAO A flavin reduction by nine α,α-[^{2}H] para-substituted benzylamine analogues and correlation with the σ substituent parameter results in a ρ value of 2.2 ± 0.4 with a correlation coefficient of 0.90 (Figure 6A, lower plot). A similar ρ value of 2.1 ± 0.5 was observed in correlations of the steady state oxidation rate of the deuterated substrate analogues (Figure 6C, lower plot).

The similarity of the ρ values with both protio and dideuterio substrates (panels A and C of Figure 6) (2.2 and 1.8, respectively) suggests α-C−H bond cleavage is the rate-limiting step in catalysis. Furthermore, this similarity suggests that the values for the deuterium kinetic isotope effects on k_{cat} and k_{red} are independent of substituent identity.

Equations describing the steady state and stopped flow rates of flavin reduction by α,α-[^{1}H] para-substituted benzylamine analogues (not including the four anomalous substituents) are

$$\log k_{red} = 2.01(\pm 0.25)\sigma + 0.57(\pm 0.06) \quad (7)$$

$$\log k_{cat} = 1.89(\pm 0.40)\sigma + 0.79(\pm 0.11) \quad (8)$$

The same equations for α,α-[^{2}H] para-substituted benzylamine analogues are

$$\log k_{red} = 2.19(\pm 0.41)\sigma - 0.4(\pm 0.1) \quad (9)$$

$$\log k_{cat} = 2.14(\pm 0.45)\sigma - 0.3(\pm 0.1) \quad (10)$$

The rate of flavin reduction by the four anomalous substrates

is best described by

$$\log k_{red} = 0.50(\pm 0.04)\sigma + 0.74(\pm 0.03) \quad (11)$$

DISCUSSION

Structure−Activity Relationships Describing the Binding of Para-Substituted Benzylamine Analogues to MAO A. The binding affinities of para-substituted benzylamine analogues for MAO A are governed by the van der Waals volume (V_w) of the substituent. Increasing substituent size results in tighter binding to the enzyme. Correction of dissociation constants to reflect the concentration of deprotonated amine present at the pH of the kinetic measurements (eq 4b) significantly improved all MAO A binding correlations. This provides further support for the selective binding of the deprotonated amine to the enzyme as originally proposed by McEwen et al. (*42*, *43*).

This correlation suggests that the enzyme contains a large binding pocket situated around the para position of the bound substrate and is consistent with the known specificity of MAO A for substrates with large aromatic ring systems such as serotonin. The finding of two separate binding correlations (eqs 5 and 6) with similar dependence upon V_w (Figure 5) is best explained by additional interactions of the para substituents with the enzyme binding site in addition to the steric effects. The properties of three of the substituents (NO_2, CF_3, and CF_3O) would suggest the formation of hydrogen bonds which would have a negative influence on binding affinity. However, this argument cannot be applied to the *tert*-butyl group.

Walker and Edmondson have conducted a similar QSAR analysis on MAO B with a smaller set of para- and meta-substituted benzylamines (*8*). Binding interactions of the para-substituted benzylamine analogues with MAO B can be described as follows (*8*):

$$\log K_d = -1.10(\pm 0.01)\pi + 0.17(\pm 0.05)V_w - 3.61(\pm 0.08) \quad (12)$$

MAO B QSAR data indicate that the binding of this class of substrate analogues to MAO B is tighter with smaller, more hydrophobic substituents. This correlation required no correction of K_d values for the concentrations of deprotonated amine. After recalculation of all MAO B K_d values using eq 4b, correlation with the hydrophobicity parameter (π) was statistically less significant, but still showed hydrophobicity to be the principal determinant of binding affinity (not shown).

Structure−Activity Relationships Describing the Rate of MAO A Flavin Reduction by Para-Substituted Benzylamine Analogues. For structure−activity relationships to be mechanistically interpretable, the measured rates must reflect the rate of C−H bond cleavage. Furthermore, this step is required to be rate-limiting with all of the benzylamine analogues that were tested. The observation of similarly large kinetic isotope effects for all the benzylamines that were tested suggests that α-C−H bond cleavage is rate-limiting under both steady state and stopped flow conditions with MAO A as found previously with MAO B (*8*).

Analysis of MAO A rate QSAR was complicated by aggregation of the enzyme at concentrations above 1 μM (Figure 2). Although this effect precluded simultaneous analysis of steady state and reductive half-reaction data, similar correlations were obtained when the data were analyzed separately. Both the steady state rates and the limiting rates of flavin reduction exhibit a positive correlation with the electronic parameter (σ). A small negative contribution of the Taft steric parameter (E_s) observed in steady state rate correlations is not considered significant due to cross-correlations between subsets of substituent parameters. Correlations of MAO A k_{cat} and/or k_{red} rates (excluding the four anomalous substituents) with σ show a positive ρ value of approximately 2.0 for both α,α-[^{1}H]- and α,α-[^{2}H]-benzylamine analogues, indicating electron-withdrawing substituents significantly enhance the rate of α-C−H bond cleavage. The increase in reaction rate is facilitated by delocalization of electron density into the benzene ring, suggesting that negative charge develops at the α-carbon in the transition state. Negative charge development in the transition state is consistent with a proton abstraction mechanism in MAO A catalysis for α-C−H bond cleavage. This result is markedly different from that observed previously with bovine liver MAO B, in which no contribution of σ to the reaction rate is observed (*8*).

The rationale for the smaller ρ values observed in rate correlations with the four substituents (Figure 6B) which did not fit with the majority of the substituents (Figure 6A) can be explained by consideration of the resonance properties of these substituents. Hammett σ substituent constants represent the sum of two separate and not necessarily equal electronic components. These include a field-inductive component that describes polarizations that occur in both through-bond and through-solvent space, and a resonance component that describes the delocalization of electron density through π orbital interactions (*23*, *45*). Thus, σ_p can be considered in the following manner:

$$\sigma_p = \alpha F' + R' \quad (13)$$

where F' is the field-inductive component, R' is the resonance component, and α is a factor whose value is empirically determined to be near unity (*23*). Reanalysis of the MAO A rate data using F' and R' in place of σ reveals correlations that may explain the behavior of the anomalous substituents.

Correlations of log k_{red} (excluding the four anomalous substituents, i.e., Figure 6A) and k_{cat} (Figure 6C) with F' and R' show an equal contribution of field-inductive and resonance effects (Table 5):

$$\log k_{red} = 1.95(\pm 0.34)R' + 2.07(\pm 0.36)F' + 0.54(\pm 0.13) \quad F_{2,9} = 28 \quad r = 0.93 \quad (14)$$

$$\log k_{cat} = 1.91(\pm 0.53)R' + 1.88(\pm 0.63)F' + 0.80(\pm 0.21) \quad F_{2,4} = 9.0 \quad r = 0.90 \quad (15)$$

In contrast, correlation of the four anomalous-behaving substituents (Figure 6B) with field-inductive and resonance parameters shows that contributions from the resonance factor (R') are more dominant than field-inductive (F') effects. Single-parameter fits with R' are superior to fits with either F' alone or R' and F' combined (Table 5):

$$\log k_{red} = 0.64(\pm 0.04)R' + 0.97(\pm 0.03) \quad (16)$$

Table 5: Correlations of the Steady State Rate of MAO A Oxidation of Para-Substituted Benzylamines (k_{cat}) and the Limiting Rate of Flavin Reduction by Para-Substituted Benzylamines (k_{red}) with Field-Inductive (F') and Resonance (R') Electronic Parameters[a]

parameter	correlation (slope)	*y*-intercept	correlation coefficient	*F*	significance
		k_{red}[b] (12 substituents)			
F'	1.77 ± 0.73	0.21 ± 0.23	0.61	5.9	0.036
R'	1.65 ± 0.69	1.01 ± 0.20	0.60	5.7	0.038
$F' + R'$	2.07 ± 0.36 1.95 ± 0.34	0.54 ± 0.13	0.93	28.4	0.0001
σ	2.01 ± 0.25	0.57 ± 0.06	0.93	62.6	<0.0001
		k_{red}[c] (4 anomolous substituents)[d]			
F'	1.53 ± 0.18	0.18 ± 0.22	0.83	6.7	0.081
R'	0.64 ± 0.04	0.97 ± 0.03	0.99	213	0.0007
$F' + R'$	0.22 ± 0.20	0.87 ± 0.10 0.58 ± 0.07	0.99	114	0.009
σ	0.50 ± 0.04	0.74 ± 0.03	0.99	170	0.001
		k_{cat} (7 substituents)			
F'	1.36 ± 1.13	0.57 ± 0.38	0.48	1.5	0.28
R'	1.56 ± 0.83	1.27 ± 0.24	0.64	3.5	0.12
$F' + R'$	1.87 ± 0.63 1.91 ± 0.53	0.80 ± 0.22	0.90	9.0	0.0331
σ	1.89 ± 0.40	0.79 ± 0.11	0.90	22.5	0.0052

[a] Correlations of k_{cat} and k_{red} utilize data from Tables 1 and 2, respectively. [b] Correlations of k_{red} determined for benzylamine analogues which exhibit a ρ value of 1.8 (Figure 6A). [c] Correlations of k_{red} determined for benzylamine analogues which exhibit a ρ value of 1.9 (Figure 6C). [d] Two data points are available for *p*-*N*,*N*-dimethylaminobenzylamine from the anaerobic rates of flavin reduction and protonated imine product formation.

Field-inductive and resonance parameters have been used to analyze reaction rate data obtained with aromatic amine dehydrogenase (*29*). The rate of reduction of aromatic amine dehydrogenase by para-substituted benzylamine analogues showed no significant correlation with the substituent electronic parameter (σ). However, a strong correlation of reaction rate with the field-inductive component (F') of σ was observed. Different contributions of field-inductive and resonance effects in MAO A catalysis likely account for the different ρ values observed with the principal analogues shown in Figure 6A and the anomalous-behaving analogues shown in Figure 6B. Despite the difference in the magnitude of ρ, both rate correlations show that electron-withdrawing groups enhance the rate of α-C−H bond cleavage of MAO A in catalysis.

Mechanistic Interpretation of Spectroscopic and QSAR Results. Anaerobic reduction of MAO A with substrate (Figure 1) and titration with the irreversible inhibitor clorgyline clearly show that the stoichiometry of the MAO A reduction is 1 mol of substrate per mole of enzyme active centers. Since the oxidation of substrate is a two-electron process and reduction of the flavin a two-electron process, there is no reason to postulate the necessity of additional redox-active groups for catalysis. Although a dithionite-reducible disulfide may be present in MAO A (*32*), these data show it is not involved in catalysis. Rapid-scanning stopped flow spectroscopy (Figure 4) demonstrates that no detectable spectral intermediates are observed during the anaerobic reduction of MAO A as observed previously with bovine liver MAO B (*41*).

Results of the QSAR analysis provide further insight into the mechanism of MAO A. The magnitudes and signs of ρ values have been used as indicators of the mechanism of C−H bond cleavage in other enzymatic systems. Hartman and Klinman observed a ρ value of 1.5 from correlations of calculated rates of cofactor reduction in bovine serum amine oxidase with the electronic substituent parameter σ (*27*), consistent with a proton abstraction mechanism in this quinoprotein. Mechanisms involving suspected hydride transfers, such as that of D-amino acid oxidase of *Trigonopsis variabilis* (*30*) and L-lactate oxidase (*31*), exhibit negative ρ values.

The large positive ρ value (2.0) observed for the oxidation of para-substituted benzylamine analogues by MAO A strongly supports a proton abstraction mechanism of α-C−H bond cleavage and thus rules out any mechanisms involving hydride transfer or hydrogen atom abstraction. Two of the proposed mechanisms for MAO catalysis, the aminium cation radical mechanism (Scheme 2) (*15*) or the polar nucleophilic mechanism shown in Scheme 3 (*17*, *18*), both involve proton abstraction steps, and therefore, either mechanism is supported by the observation of a positive ρ value. The failure to observe spectral evidence for intermediates such as a flavin radical or a flavin 4a adduct also does not provide a means for discriminating between these two mechanistic possibilities since these intermediates may form at a concentration that is too low for them to be spectrally observable.

If the aminium cation radical mechanism (Scheme 2) is operative in MAO A catalysis, electronic (σ) effects might be observed on both the amininium radical formation and the rate-limiting α-C−H bond cleavage. In model studies of *N*,*N*-dimethylbenzylamine oxidation by one-electron oxidizing agents such as alkaline ferricyanide (*46*) or chlorine dioxide (*47*−*49*), the rate-limiting step is electron abstraction from the amine nitrogen and is characterized by negative ρ values of unity. Proton transfer from the α-carbon of a positively charged aminium radical to produce a resonance structure with no net charge would be consistent with a positive ρ value. A positive value of ρ (1.7) is observed for the rate-limiting proton transfer from *N*,*N*-dimethylaniline cation radicals to acetate anion in acetonitrile (*50*).

Although an aminium cation radical mechanism is consistent with the observation of a positive ρ value, this mechanism raises several other concerns regarding its validity. The major problem is the identity of the one-electron oxidant on the enzyme required to generate the aminium cation radical. The thermodynamic improbability of a ground state flavin ($E_m \sim -0.2$ to 0 V) as the oxidant for a primary amine ($E_m = 1.5$ V) has previously been emphasized (*8*). Additionally, the failure to observe any flavin semiquinone during rapid-scanning or single-wavelength stopped flow experiments with MAO B (*8*, *41*) or MAO A (Figure 4) where C−H bond cleavage is rate-limiting is in accord with this prediction. The possibility of a protein-bound semiquinone being the oxidizing species has been considered (*20*, *22*). However, no detectable EPR signals are found in either purified recombinant MAO A or purified recombinant MAO B (P. A. Newton-Vinson, R. K. Nandigama, and D. E. Edmondson, unpublished data). Thus, the absence of an identifiable one-electron oxidant on either MAO A or MAO B capable of performing the initial single-electron oxidation of the amine substrate makes the aminium cation radical mechanism, in our opinion, improbable.

The polar nucleophilic mechanism depicted in Scheme 3 (*17*) relies on the electrophilicity of the oxidized flavin 4a position (*51*). Model reactions of *N*(5)-ethyllumiflavinium

salts with para-substituted benzylamine analogues suggest that the rate of benzylamine−flavin 4a adduct formation is faster than the rate of α-C−H bond cleavage (*19*). Electron-withdrawing para substituents were observed to increase the limiting rate of aldimine formation ($\rho = 0.8$), consistent with negative charge development during α-C−H bond cleavage (*19*). However, several kinetic and chemical observations are inconsistent with this mechanism (Scheme 3). The absence of any spectroscopically detectable flavin 4a adduct (Figure 4) in either MAO A or MAO B is of concern since it must be formed prior to the rate-limiting C−H bond cleavage step (Scheme 3). A second prediction of the polar group transfer mechanism in Scheme 3 is that a smaller apparent kinetic isotope effect should be observed on the rate of flavin bleaching relative to that observed in steady state measurements. The loss of oxidized flavin absorbance in reductive half-reaction experiments should be a composite of amine−flavin 4a adduct formation (no kinetic isotope effect) and flavin reduction (large kinetic isotope effect). The steady state and stopped flow kinetic isotope effect data (Tables 1 and 2, respectively) show nearly identical values over a broad range of rates. Similarly, the observed kinetic isotope effects on the rate of flavin reduction by *p-N,N*-dimethylaminobenzylamine and the formation of the protonated imine product ($\lambda_{max} = 390$ nm) (*2*) are identical (Table 2). These results do not support the formation of any significant levels of flavin 4a adducts in the MAO A-catalyzed oxidation of this substrate class. An additional concern with the mechanism depicted in Scheme 3 is the identity of the base responsible for abstracting the benzyl proton from the flavin 4a adduct. The pK_a of this benzylic proton [∼30−35 in benzylamine (*52*), perhaps lower in a 4a adduct] is higher than that of known amino acid bases. Furthermore, the large isotope effects observed on α-C−H bond cleavage suggest that the difference in the pK_a values between the α-methylene proton and the H acceptor is small (*53*), arguing against an amino acid residue as a participating base.

A reformulation of the mechanism shown in Scheme 3 that is more consistent with the kinetic and spectroscopic data is proposed in Scheme 4. Formation of a flavin 4a adduct is proposed to occur as shown in Scheme 3. The formation of this 4a-alkylated isoalloxazine ring leads to a very strong base at N(5) of the flavin with a pK_a that is expected to be in the range of anilines (pK_a of ∼30) (*54*). Thus, a concerted transfer of the benzyl proton to N(5) of the 4a-alkyl flavin should be facilitated. Following this concerted addition−α-C−H bond cleavage reaction, elimination would occur, producing the experimentally observed protonated imine product (data not shown) and the reduced flavin cofactor which is reoxidized by O_2. This reformulation of the polar nucleophilic mechanism would be in agreement with most existing model and enzymatic mechanistic data and is amenable to further experimental verification.

Comparison of MAO A and MAO B QSAR Results. The influence of para substitution on rates of flavin reduction differ significantly for MAO A and MAO B. The rates of bovine liver MAO B oxidation of para-substituted benzylamine analogues are influenced mainly by the Taft steric parameter (E_s) (*8*) with no observable dependence on the electronic parameter (σ). In contrast, MAO A oxidation rates for the same class of substrate analogues exhibit a strong dependence on the electron-withdrawing properties of the

Scheme 4: Proposed Concerted Polar Nucleophilic Mechanism for MAO A Catalysis

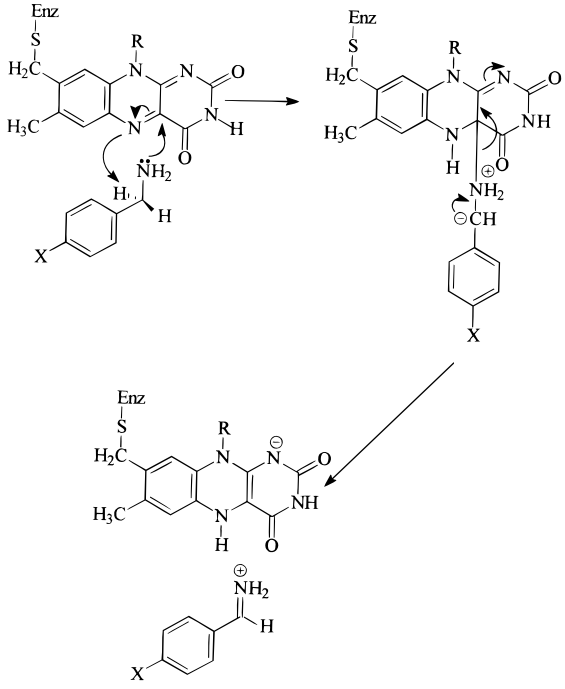

para substituent. This difference in behavior between two similar enzymes whose sequences are 71% identical and whose cofactor structures are identical is, to our knowledge, unprecedented. The possibility that the two enzymes function by differing mechanisms of α-C−H bond cleavage cannot be ruled out but is considered unlikely. This situation presents a clear distinction between the two enzymes and also presents a test of the utility of structure−activity relations as probes of enzyme mechanisms.

Possibile explanations for this differential behavior are presented below which may provide tests for future investigations. One possibility is that the two enzymes differ in the extent of H^+ abstraction in the transition state for the mechanism shown in Scheme 2. In the case of MAO B, H^+ abstraction from the cation radical would occur early in the transition state and the negative charge formation on the benzyl would be offset by the positive charge genetated on the amine nitrogen so that the benzyl carbon would possess mostly radical character. The situation with MAO A could be explained by H^+ abstraction later in the transition state such that the negative charge development on the benzyl carbon would be more sensitive to the nature of the para substituent. This scenario, of course, is dependent on the demonstration that the cation radical mechanism is operative in MAO catalysis which is considered unlikely in the absence of an identifiable one-electron oxidant for the amine.

Another possible explanation for the observed difference in rate QSAR is that the configuration of benzylamine analogues bound to MAO B may not facilitate the overlap of the π-orbitals of the benzene ring with the developing π-orbital of the α-C−H bond being broken. If this situation occurs, stabilization of the developing negative charge density on the benzyl carbon would be unaffected by the electronic effects transmitted through the aromatic ring, resulting in the observation of a small or nearly zero ρ value (Figure 7). An example of this situation in a nonenzymatic

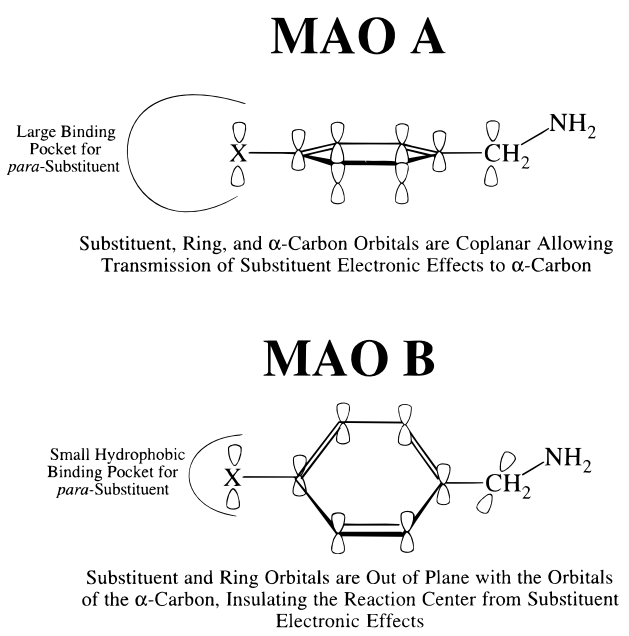

FIGURE 7: Model representation of the relative conformations of para-substituted benzylamine analogues bound to recombinant human liver MAO A and to bovine liver MAO B.

system has been provided by Bordwell et al. (*55*). Consistent with this hypothesis is the *absence* of substituent electronic effects on the *binding* of benzylamine analogues to bovine liver MAO B (*8*), whereas they are present in the case of MAO A (see eq 4b and the discussion above). In contrast to the absence of electronic effects in the binding of benzylamine analogues to MAO B, QSAR studies of the binding of the competitive inhibitors (*N*,*N*-dimethylbenzylamine and α-methylbenzylamine) to this enzyme demonstrate the participation of para electronic effects on amine deprotonation in facilitating the binding affinities (*56*). Presumably, these benzylamine analogues are bound to the enzyme in a manner where steric effects do not influence the transmission of electronic effects to the benzyl carbon from the aryl para position. These considerations suggest the steric alignment of the aryl ring and the alkylamine moieties in MAO B-bound benzylamine analogues either reduces or eliminates the electronic influence of para substituents.

The distinction between these two alternative requires more definitive experimental approaches. Not only are there clear differences between the two enzymes that may be important for future drug development, but this work should also serve as a guide to other workers using QSAR approaches as a mechanistic probe in enzyme systems. Care should be taken in mechanistic interpretations of systems that exhibit an absence of substituent electronic effects on rate.

ACKNOWLEDGMENT

We thank Dr. Walter Weyler for the gift of the MAO A-expressing yeast strain and Dr. R. K. Nandigama of this laboratory for performing the enzyme-monitored turnover experiments. Access to the OLIS-RSM1000 rapid-scanning stopped flow spectrophotometer was kindly provided by Dr. David Wilson (Georgia State University).

REFERENCES

1. Weyler, W., Hsu, Y. P., and Breakefield, X. O. (1990) *Pharmacol. Ther. 47*, 391.
2. Edmondson, D. E., Bhattacharyya, A. K., and Walker, M. C. (1993) *Biochemistry 32*, 5196.
3. Woo, J. C. G., and Silverman, R. B. (1995) *J. Am. Chem. Soc. 117*, 1663.
4. Berry, M. D., Juorio, A. V., and Paterson, I. A. (1994) *Prog. Neurobiol. 42*, 375.
5. Bach, A. W., Lan, N. C., Johnson, D. L., Abell, C. W., Bembenek, M. E., Kwan, S. W., Seeburg, P. H., and Shih, J. C. (1988) *Proc. Natl. Acad, Sci. U.S.A. 85*, 4934.
6. Kearney, E. B., Salach, J. I., Walker, W. H., Seng, R. L., Kenney, W., Zeszotek, E., and Singer, T. P. (1971) *Eur. J. Biochem. 24*, 321.
7. Olanow, C. W. (1993) *Adv. Neurol. 60*, 666.
8. Walker, M. C., and Edmondson, D. E. (1994) *Biochemistry 33*, 7088.
9. Ramsay, R. R. (1991) *Biochemistry 30*, 4624.
10. Husain, M., Edmondson, D. E., and Singer, T. P. (1982) *Biochemistry 21*, 595.
11. Strickland, S., Palmer, G., and Massey, V. (1975) *J. Biol. Chem. 250*, 4048.
12. Weyler, W., and Salach, J. I. (1985) *J. Biol. Chem. 260*, 13199.
13. Tan, A. K., and Ramsay, R. R. (1993) *Biochemistry 32*, 2137.
14. Ramsay, R. R., Sablin, S. O., Bachurin, S. O., and Singer, T. P. (1993) *Biochemistry 32*, 9025.
15. Silverman, R. B., Hoffman, S. J., and Catus, W. B., III (1980) *J. Am. Chem. Soc. 102*, 7126.
16. Silverman, R. B. (1992) in *Advances in Electron Transfer Chemistry* (Mariano, P., Ed.) p 177, JAI Press, Inc., Greenwich, CT.
17. Brown, L. E., and Hamilton, G. R. (1970) *J. Am. Chem. Soc. 92*, 7225.
18. Kim, J., Bogdan, M. A., and Mariano, P. S. (1993) *J. Am. Chem. Soc. 115*, 10591.
19. Hoegy, S. E., and Mariano, P. S. (1997) *Tetrahedron 53*, 5027−5046.
20. Edmondson, D. E. (1995) *Xenobiotica 25*, 735.
21. Edmondson, D. E. (1996) in *Flavins and Flavoproteins 1996* (Stevenson, K. J., Massey, V., and Williams, C. H., Jr., Ed.) pp 23−24, University of Calgary Press, Calgary, AB.
22. DeRose, V. J., Woo, J. C., Hawe, W. P., Hoffman, B. M., Silverman, R. B., and Yelekci, K. (1996) *Biochemistry 35*, 11085.
23. Hansch, C., and Leo, A. (1995) *Exploring QSAR. Fundamentals and Applications in Chemistry and Biology*, American Chemical Society, Washington, DC.
24. Fujita, T., Iwasa, J., and Hansch, C. (1964) *J. Am. Chem. Soc. 86*, 5176.
25. Bondi, A. (1964) *J. Phys. Chem. 68*, 441.
26. Hansch, C., Leo, A., and Hoekman, D. (1995) *Exploring QSAR. Hydrophobic, Electronic, and Steric Constants*, American Chemical Society, Washington, DC.
27. Hartmann, C., and Klinman, J. P. (1991) *Biochemistry 30*, 4605.
28. Davidson, V. L., Jones, L. H., and Graichen, M. E. (1992) *Biochemistry 31*, 3385.
29. Hyun, Y. L., and Davidson, V. L. (1995) *Biochemsitry 34*, 816.
30. Pollegioni, L., Blodig, W., and Ghisla, S. (1997) *J. Biol. Chem. 272*, 4924.
31. Yorita, K., Janko, K., Aki, K., Ghisla, S., Palfey, B. A., and Massey, V. (1997) *Proc. Natl. Acad. Sci. U.S.A. 94*, 9590.
32. Sablin, S. O., and Ramsay, R. R. (1998) *J. Biol. Chem. 273*, 14074.
33. Weyler, W., Titlow, C. C., and Salach, J. I. (1990) *Biochem. Biophys. Res. Commun. 173*, 1205.
34. Tan, A. K., Weyler, W., Salach, J. I., and Singer, T. P. (1991) *Biochem. Biophys. Res. Commun. 181*, 1084.
35. Nystrom, R. F. (1955) *J. Am. Chem. Soc. 77*, 2544.
36. Bright, H. J., and Porter, D. J. T. (1975) *Enzymes (3rd Ed.) 12*, 421.
37. Matheson, I. B. C. (1990) *Comput. Chem. 14*, 49.
38. Hille, R., and Massey, V. (1982) *J. Biol. Chem. 257*, 8898.
39. Klinman, J. P., and Matthews, R. G. (1985) *J. Am. Chem. Soc. 107*, 1058.

40. Northrop, D. B. (1975) *Biochemistry 14*, 2644.
41. Miller, J. R., Edmondson, D. E., and Grissom, C. B. (1995) *J. Am. Chem. Soc. 117*, 7830.
42. McEwen, C. M., Sasaki, G., and Lenz, W. R. (1968) *J. Biol. Chem. 243*, 5217.
43. McEwen, C. M., Jr., Sasaki, G., and Jones, D. C. (1969) *Biochemistry 8*, 3952.
44. Blackwell, L. F., Fischer, A., Miller, I. J., Topsom, R. D., and Vaughan, J. (1964) *J. Chem. Soc.*, 3588.
45. Swain, C. G., and Lupton, E. C., Jr. (1968) *J. Am. Chem. Soc. 90*, 4328.
46. Audeh, C. A., and Smith, J. R. L. (1971) *J. Chem. Soc. B*, 1280.
47. Rosenblatt, D. H., Hull, L. A., DeLuca, D. C., Davis, G. T., Weglein, R. C., and Williams, H. K. R. (1967) *J. Am. Chem. Soc. 89*, 1158.
48. Hull, L. A., Davis, G. T., Rosenblatt, D. H., Williams, H. K. R., and Weglein, R. C. (1967) *J. Am. Chem. Soc. 89*, 1163.
49. Hull, L. A., Rosenblatt, D. H., and Mann, C. K. (1969) *J. Phys. Chem. 73*, 2142.
50. Parker, V. D., and Tilset, M. (1991) *J. Am. Chem. Soc. 113*, 8778.
51. Bruice, T. C. (1976) in *Progress in Bioorganic Chemistry* (Kaiser, E. T., and Kezdy, F. J., Eds.) pp 1−88, John Wiley and Sons, New York.
52. Streitwieser, A. J., Juarustu, E., and Nebenzahl, L. L. (1980) in *Comprehensive Carbanion Chemistry* (Buncel, E., and Durst, T., Eds.) pp 323−381, Elsevier, Amsterdam.
53. Bell, R. P. (1973) *The Proton in Chemistry*, Cornell University Press, Ithaca, NY.
54. Chan, T. W., and Bruice, T. C. (1978) *Biochemistry 17*, 4784.
55. Bordwell, F. G., Cheng, J. P., Satish, A. V., and Twyman, C. L. (1992) *J. Org. Chem. 57*, 6542.
56. Edmondson, D. E. (1999) *Drug Metab. Rev. 31*, 235.

BI990920Y